

Human-Driven Runoff Decline and Hydrological Drought Intensification in Semi-arid Regions in the Last 40 Years Revealed by a Hybrid Physics-Deep Learning Framework

To intuitively analyze the impacts of climate variables on hydrological drought, we employed SHAP (SHapley Additive exPlanations) analysis to evaluate the contribution ranking of these variables (Fig S1). According to the results obtained, potential evapotranspiration emerged as the primary climatic factor influencing hydrological processes in the study area, followed by snowmelt, temperature, and precipitation.

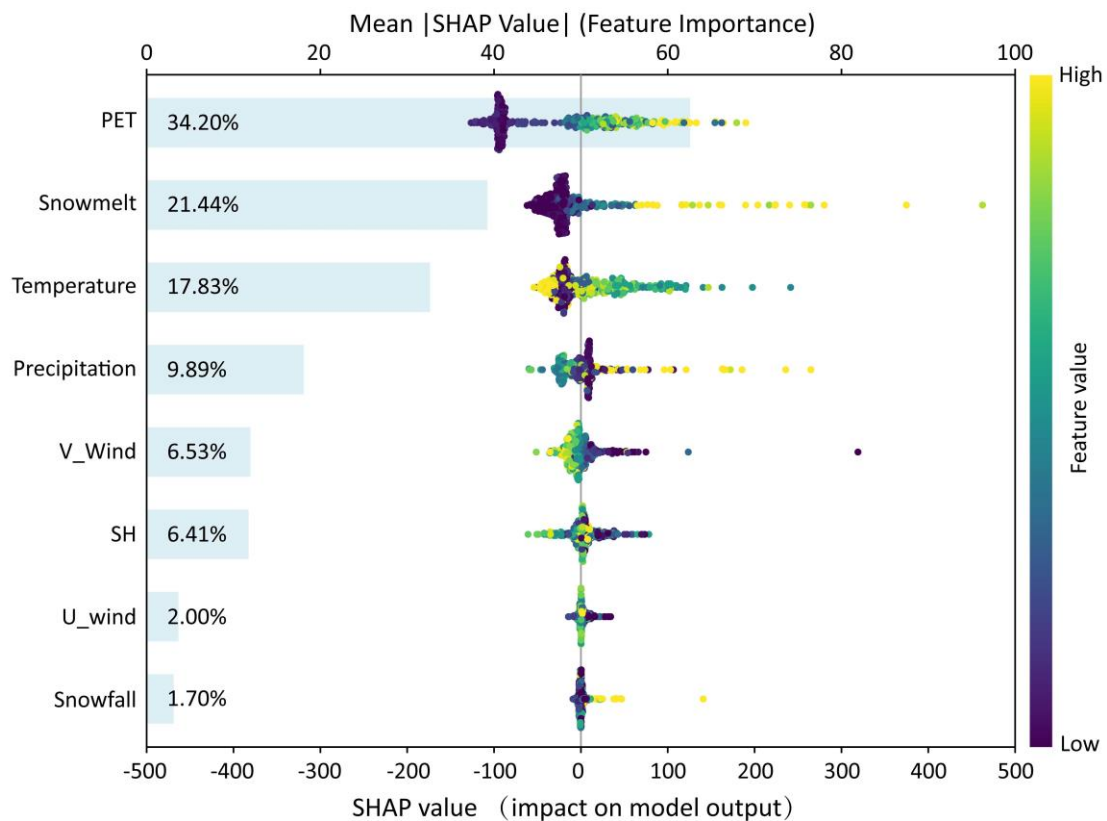


Fig. S1. Contribution ranking of climate variables to hydrological drought impacts.

Note: Contribution ranking from high to low: potential evapotranspiration, snowmelt, temperature, precipitation, V-wind, heat flux, U-wind, snowfall.

Fig. S2 shows the long-term trend in snow water equivalent (SWE) in the Xilin River

Basin during 1980–2020. The results indicate that SWE exhibits a significant decreasing trend at a rate of -1.27 mm/a.

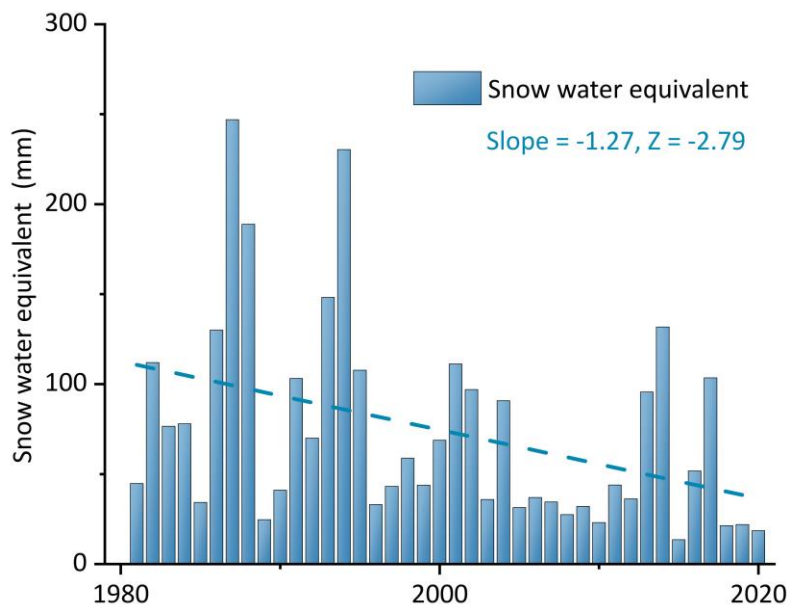


Fig. S2. Trend in snow water equivalent (SWE) in the Xilin River Basin during 1980–2020.

Fig. S3 illustrates land-use conversions in the study area over the past two decades. In 2000, grassland dominated the Xilin River Basin (accounting for 91%), while forest and cropland occupied only 0.81% and 2.77%, respectively (Fig. 10). Between 2000–2010, the watershed underwent land use transformation dominated by ecological restoration: high-coverage grassland area increased by 5.04%, while cropland decreased relatively by 8.30%. Most strikingly, forest area surged from 30.87 km² to 158.16 km² (a 412.3% increase). This change primarily resulted from government-implemented policies of returning farmland to forest and afforestation during this period. Ecological restoration projects improved watershed ecology, but rapid forest expansion simultaneously enhanced vegetation transpiration. From 2011–2020, local government actively promoted agriculture and economic development, with cropland and built-up land increasing relatively by 14.89% and 19.83%, respectively.

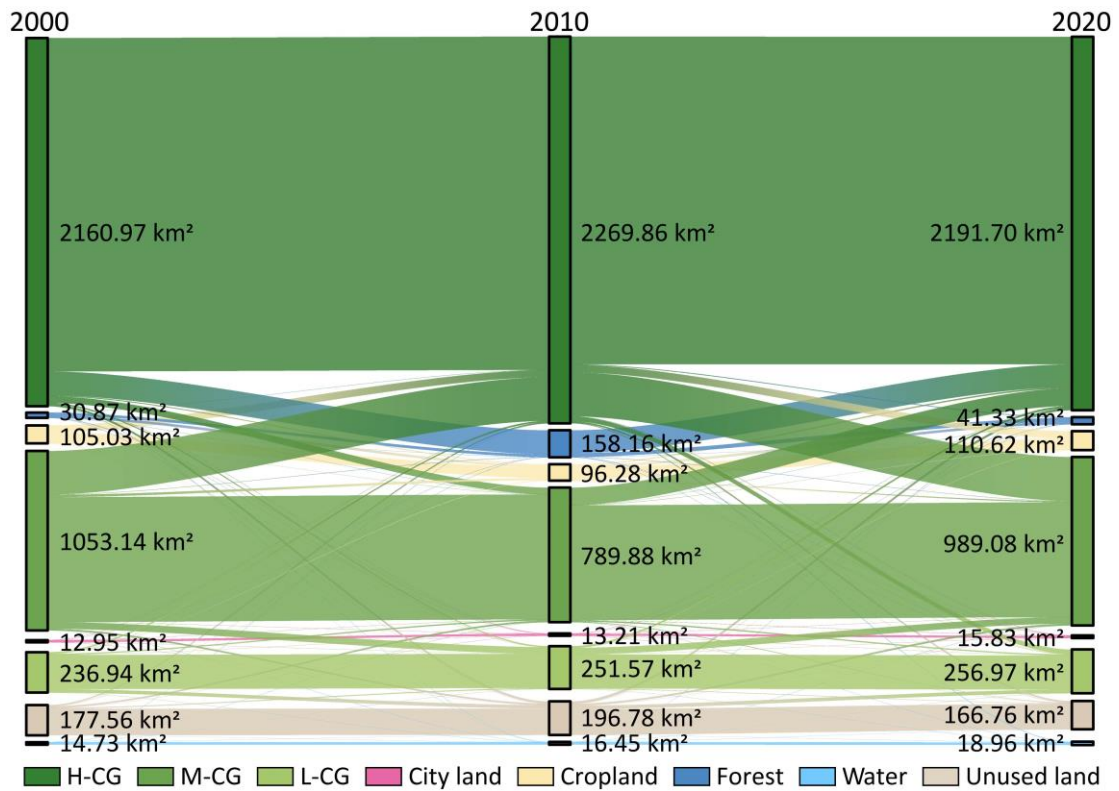


Fig. S3. Land use type transitions during 2000–2010–2020.

Over the past 40 years, human water withdrawal, sheep population, and grazing intensity have all exhibited significant upward trends at rates of $0.13 \times 10^4 \text{ m}^3/\text{km}^2/\text{a}$, $0.26 \times 10^4 \text{ head}/\text{a}$, and $0.02 \text{ SU}/\text{ha}/\text{a}$, respectively (Fig. S4). Comparing the baseline and altered periods, water withdrawal intensity increased from $9.48 \times 10^4 \text{ m}^3/\text{km}^2$ to $12.31 \times 10^4 \text{ m}^3/\text{km}^2$ (an increase of 29.9%), sheep population surged from $4.52 \times 10^4 \text{ head}$ to $10.29 \times 10^4 \text{ head}$ (an increase of 127.7%), and grazing intensity rose from 0.26 SU/ha to 0.61 SU/ha (an increase of 134.6%).

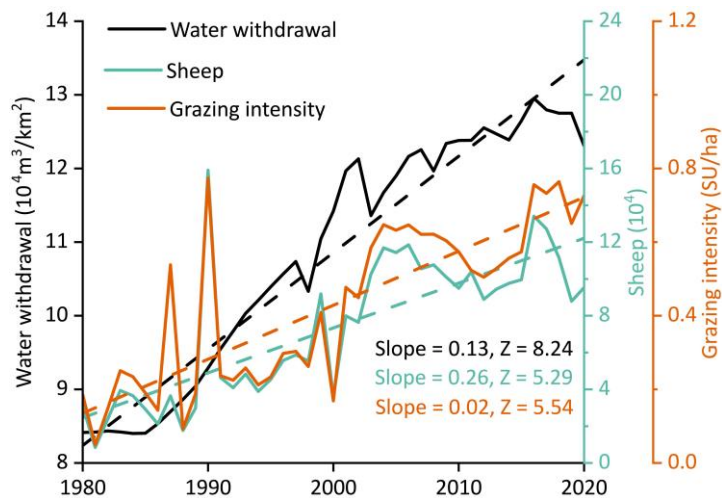


Fig. S4. Trends in human water withdrawal, sheep population, and grazing intensity from 1980–2020.